8820–8832 *Nucleic Acids Research, 2011, Vol. 39, No. 20* *Published online 29 September 2011*
doi:10.1093/nar/gkr650

Structural basis for nematode eIF4E binding an $m^{2,2,7}$G-Cap and its implications for translation initiation

Weizhi Liu[1], Marzena Jankowska-Anyszka[2], Karolina Piecyk[1,2], Laura Dickson[1], Adam Wallace[1], Anna Niedzwiecka[3,4], Janusz Stepinski[3], Ryszard Stolarski[3], Edward Darzynkiewicz[3], Jeffrey Kieft[1], Rui Zhao[1], David N. M. Jones[5,*] and Richard E. Davis[1,*]

[1]Department of Biochemistry and Molecular Genetics, University of Colorado School of Medicine, Aurora, CO 80045, USA, [2]Faculty of Chemistry, Department of Organic Chemistry, University of Warsaw, 02-093 Warsaw, [3]Division of Biophysics, Institute of Experimental Physics, Faculty of Physics, University of Warsaw, 02-089 Warsaw, [4]Laboratory of Biological Physics, Institute of Physics, Polish Academy of Sciences, 02-668 Warsaw, Poland and [5]Department of Pharmacology, University of Colorado School of Medicine, Aurora, CO 80045, USA

Received June 6, 2011; Revised July 10, 2011; Accepted July 23, 2011

ABSTRACT

Metazoan spliced leader (SL) *trans*-splicing generates mRNAs with an $m^{2,2,7}$G-cap and a common downstream SL RNA sequence. The mechanism for eIF4E binding an $m^{2,2,7}$G-cap is unknown. Here, we describe the first structure of an eIF4E with an $m^{2,2,7}$G-cap and compare it to the cognate m^7G-eIF4E complex. These structures and Nuclear Magnetic Resonance (NMR) data indicate that the nematode *Ascaris suum* eIF4E binds the two different caps in a similar manner except for the loss of a single hydrogen bond on binding the $m^{2,2,7}$G-cap. Nematode and mammalian eIF4E both have a low affinity for $m^{2,2,7}$G-cap compared with the m^7G-cap. Nematode eIF4E binding to the m^7G-cap, $m^{2,2,7}$G-cap and the $m^{2,2,7}$G-SL 22-nt RNA leads to distinct eIF4E conformational changes. Additional interactions occur between Ascaris eIF4E and the SL on binding the $m^{2,2,7}$G-SL. We propose interactions between Ascaris eIF4E and the SL impact eIF4G and contribute to translation initiation, whereas these interactions do not occur when only the $m^{2,2,7}$G-cap is present. These data have implications for the contribution of 5′-UTRs in mRNA translation and the function of different eIF4E isoforms.

INTRODUCTION

Eukaryotic translation initiation is the main regulatory step for translation and is controlled at multiple levels (1–3). The initiation complex eIF4F mediates ribosome recruitment to mRNA and is composed of three subunits: eIF4E, eIF4G and eIF4A (4). The binding of eIF4E to the cap is an essential step for cap-dependent translation (4–6). Efficient mRNA translation initiation also requires the scaffold protein, eIF4G, which interacts with eIF4E, eIF4A, the mRNA, and recruits the 40 S ribosome complex to generate the translation initiation complex (2–5).

The binding affinity of eIF4E for the mRNA cap is considered to play a key role in translation efficiency (7,8). In nematodes, two different types of capped mRNA are present, m^7G- and $m^{2,2,7}$G-cap. A large percentage of nematode mRNAs are matured by spliced leader RNA *trans*-splicing which generates the mature 5′-ends of mRNAs through the addition of a short leader sequence, the 22-nt spliced leader (SL), and a new cap (an $m^{2,2,7}$G-cap in metazoa) (9–12). Previous studies suggest that some nematode eIF4E isoforms (*Ascaris suum* eIF4E-3 and Caenorhabditis *elegans* eIF4E-1, -2, -5) are able to recognize the two different nematode mRNA caps (10,13–15). Current data suggest that most eIF4E proteins have a strong preference for the m^7G-cap compared with an $m^{2,2,7}$G-cap evident from (i) their higher binding affinity for the m^7G-cap (16) and (ii) inefficient translation of

*To whom correspondence should be addressed. Tel: + 303 724 3226; Fax: 303 724 3215; Email: richard.davis@ucdenver.edu
Correspondence may also be addressed to David N. M. Jones. Tel: + 303 724 3600; Fax: 303 724 3663; Email: david.jones@ucdenver.edu
Present address:
Weizhi Liu, Department of Pharmacology, Yale University School of Medicine, 333 Cedar Street, SHM B-302, New Haven, CT 06520, USA.

© The Author(s) 2011. Published by Oxford University Press.
This is an Open Access article distributed under the terms of the Creative Commons Attribution Non-Commercial License (http://creativecommons.org/licenses/by-nc/3.0), which permits unrestricted non-commercial use, distribution, and reproduction in any medium, provided the original work is properly cited.

$m^{2,2,7}$G-capped mRNAs in wheat germ and rabbit reticulocyte lysates (17,18). In contrast, a single nematode eIF4E isoform can translate both m^7G- and $m^{2,2,7}$G-capped mRNAs in a nematode *in vitro* translation system (17). Efficient translation of nematode $m^{2,2,7}$G-capped mRNAs requires the downstream *trans*-spliced leader (10,12,17).

Trans-splicing is an essential process in nematodes (19). Importantly, many parasitic nematodes and flatworms have *trans*-spliced mRNAs with $m^{2,2,7}$G-caps. These parasites remain a significant public health problem infecting over 2 billion people (20). Consequently, knowledge of the fundamental differences in nematode mRNA translation and the associated proteins may lead to the directed development of compounds that can specifically block parasite, but not human, gene expression.

Structural studies on the eIF4E-m^7G-cap complex have revealed the details of eIF4E interactions with the m^7G-cap (16,21–28). However, the mechanism of eIF4E binding to the atypical $m^{2,2,7}$G-cap has not been determined. It has been proposed that the observed lower affinity of mammalian eIF4E for the $m^{2,2,7}$G-cap is the consequence of a narrower binding pocket (14) or steric hindrance caused by the addition of two methyl groups at the N^2 position (29). Alternatively, intrinsic protein conformational flexibility may be a major determinant that enables the eIF4E from a *trans*-splicing flatworm to bind both caps (30).

Here, we have used a combination of X-ray crystallography, Nuclear Magnetic Resonance (NMR) spectroscopy and other biophysical techniques to examine the interaction of nematode eIF4E with the $m^{2,2,7}$G-cap. Our structural analyses represent a first step in understanding the structural specificity of eIF4E proteins for different caps and rational drug design against a parasitic nematode eIF4E. We present the first structure of an eIF4E-$m^{2,2,7}$G complex and demonstrate how the addition of two methyl groups at the N^2 position disrupts a critical hydrogen bond that is required for higher affinity binding of the m^7G-cap. NMR analyses with nematode eIF4E and its interaction with m^7G-cap, $m^{2,2,7}$G-cap and $m^{2,2,7}$G-SL demonstrate distinct conformational changes on binding these ligands. Notably, conformational changes associated with binding the $m^{2,2,7}$G-cap are significantly reduced compared with binding the m^7G-cap. Compensatory conformational changes on binding $m^{2,2,7}$G-SL provide one explanation for the requirement of the 22-nt SL RNA sequence in nematode translation of $m^{2,2,7}$G-capped, *trans*-spliced mRNAs. Our studies suggest that eIF4E proteins may undergo distinct conformational changes on binding a cap, and eIF4E interactions with the mRNA 5′-UTR could be important for the translation of some mRNAs.

MATERIAL AND METHODS

Synthesis of cap analogs and capped spliced leader sequence

Cap analogs and the $m^{2,2,7}$GTP-Sepharose affinity resin were synthesized as previously described (31–33). The $m^{2,2,7}$G-capped spliced leader sequence was prepared from a chemically synthesized 5′ phosphorylated RNA oligonucleotide, p-GGUUUAAUUACCCAAGUU UGAG (TriLink BioTechnologies, Inc.) by coupling with an imidazolide derivative of $m^{2,2,7}$GDP under aqueous conditions. Final products were isolated from the reaction mixture and purified using High Performance Liquid Chromatography (HPLC) (a detailed protocol will be published elsewhere). bn^2m^7GMP was synthesized from N^2-fluoro-2′,3′,5′-*O*-triacetyl-O^6-[2-(4-nitrophenyl)ethyl]) guanosine (34) by nucleophilic substitution with benzyl iodide, subsequent 5′-phosphorylation using the standard method of Yoshikawa (35) and the methylation carried out as previously described (31). A detailed method for the synthesis of the compound will be described elsewhere.

Protein purification

Ascaris eIF4E-3 protein was prepared from bacterial cultures induced with 0.2 mM IPTG at $A_{600} = 0.7$ and incubated overnight at 25°C. The cells were collected by centrifugation at 4000 *g*, suspended in HEPES binding buffer (20 mM HEPES, pH 7.4, 100 mM KCl, 1 mM dithiothreitol, 1 mM EDTA), sonicated and clarified by centrifugation at 16 000 *g*. The supernatant was loaded onto m^7GTP-Sepharose resin (GE Healthcare) and rotated at 4°C for 2 h. The resin was washed with the binding buffer, and eIF4E was eluted with 2 M KCl in binding buffer. The eluted protein was applied to a Superdex 75 (GE Healthcare) column equilibrated in binding buffer, and monomeric protein was collected, analyzed by Sodium Dodecyl Sulfate Polyacrylamide Gel Electrophoresis (SDS–PAGE) and concentrated using an Amicon 10 000 MW Ultra Centrifugal Filter Device (Millipore, Billerica, MA, USA).

Full-length human eIF4E was subcloned into pGEX6P-1 (GE Healthcare, Parsipanny, NJ, USA) and then transformed into *Escherichia coli* strain XA90. Protein expression was induced, the cells were collected and sonicated, and the supernatant was recovered as described above except that phosphate-buffered saline buffer was used. The cell lysate was incubated with Glutathione-Sepharose 4B (GE Healthcare) for 4 h at 4°C with rotation. The resin was washed with phosphate-buffered saline buffer, and eIF4E was cleaved from the glutathione *S*-transferase fusion protein by incubation with PreScission Protease at 4°C overnight. Eluted protein was further purified as described above on a Superdex 75 column.

Crystallization conditions, data collection and refinement

Purified *A. suum* eIF4E-$3_{(49–236)}$ was concentrated to 10 mg/ml (Amicon, 10 000 MW Ultra Centrifugal Filter Device, Millipore, Billerica, MA, USA) and then incubated with 1 mM 4E-BP peptide (RIIYDRKFLMECRNSPV, corresponding to the residues 51–67 of the human 4E-BP1 sequence) and 0.5 mM m^7G or $m^{2,2,7}$G-cap at 4°C for 1 h before crystallization setup using the hanging drop vapor diffusion method. Needle-like crystals developed in 20% MME PEG 2000, 0.2 M $(NH_4)_2SO_4$ and 100 mM Na $C_3H_5O(COO)_3$ (pH 5.6) at 4°C within 1 week using 0.5 ml 1 M NaCl as the well solution (30). Before data collection, the crystal was transferred into the equivalent mother solution containing 30% MMG

PEG 2000 for 15 min, and then flash cooled in liquid nitrogen. X-ray diffraction data were collected using the Advanced Light Source beamline 4.2.2 at the Lawrence Berkley National Laboratory and 19-ID of the Structural Biology Center, Advanced Photon Source (APS) at Chicago. The Ascaris eIF4E-3 complex structures were solved by molecular replacement using PDB:2V8W as the initial model and the program PHASER in the CCP4 suite (36). Model building and manual refinement were performed in COOT (37) and REFMAC from the CCP4 suite (36), respectively. Figures were generated using Pymol (38). At the final stage of refinement, the TLS refinement with REFMCA was used using the TLS parameter generated by the TLSMD server (39).

NMR spectroscopy

All NMR spectra were acquired on a 900 or 800 MHz Varian spectrometer at a probe temperature of 25°C. For the backbone assignment, standard 3D resonance NMR experiments were conducted including HNCACB, HNCOCA, HNCOCACB, CCONH-TOCSY using 0.5 mM triple-labeled Ascaris eIF4E-3 in complex with m^7GTP at a 1:1.2 molar ratio. The HNCACB and CBCACONH were recorded to facilitate resonance assignments for the $m^{2,2,7}$GTP complex using 0.6 mM $^{13}C/^{15}N$ Ascaris eIF4E-3. Titration experiments with $m^{2,2,7}$GTP were used to facilitate apo-form backbone assignments. Titration experiments were performed at the protein concentration of 50 μM in the presence of different molar ratios of ligands. All the NMR data were processed using NMRPipe (40) and analyzed using CcpNmr (41).

In vitro translation

In vitro translation and depletion/reconstitution assays were carried out as previously described (17). eIF4F complex consisting of full-length eIF4G and wild-type or mutant eIF4E were co-expressed and the complex purified using His-tagged eIF4G (17). eIF4F complex addition was normalized to both eIF4E and eIF4G using antibodies directed to the Ascaris proteins. Preparation and use of an optimized cap-dependent rabbit reticulocyte lysate translation system was done as described (42).

Isothermal titration calorimetry

The calorimetric titration was carried out at 20°C using a VP-ITC calorimeter (MicroCal Inc., Northampton, MA, USA). eIF4E proteins were purified as described above and used for ITC in 20 mM HEPES (pH 7.4), 1 mM EDTA and 100 mM KCl buffer. Each titration experiment consisted of a 5 μl injection followed by 29 injections of 10 μl of cap analogs. Data were processed using the single binding site model in Origin (Version 7.0 MicroCal). Control titration experiments demonstrated that the dilution heat was trivial compared with the real binding heat (e.g. buffer titrated into protein and cap titrated into buffer; data not shown).

Fluorescence titration

Titrations of eIF4E-3 with the cap analogs were performed as described previously (16). Absorption and emission spectra were recorded on Lambda 20 UV/VIS and LS-55 (Perkin-Elmer, CT, USA) spectrometers, respectively. The protein solution was spun down at 18 000 *g* for 10 min at 4°C before the experiments to remove any possible precipitants. The measurements were carried out in 50 mM HEPES/KOH, pH 7.20 ± 0.02, 200 mM KCl, 1 mM DTT and 0.5 mM EDTA, at a temperature of 20°C and repeated multiple times at eIF4E-3 concentrations of 0.4–0.6 μM. The samples of $m^{2,2,7}$GpppG used for determination of the binding constant were synthesized in seven independent batches. The temperature was controlled to ±0.2 K with a thermocouple inside the thermostated cuvette, and the sample was stirred magnetically. The fluorescence, excited at 280 nm (slit 2.5 nm, auto cut-off filter), was monitored at 335 nm (slit 2.5–4 nm, 290 nm cut-off filter), with an integration time of 30 s and a gap of 30 s for adding the cap analogue. Dilution during the titration did not exceed 2.5%. Fluorescence intensity was corrected for the inner filter effect. The emission of the free cap analogues was explicitly included in the numerical analysis. A theoretical curve for the fluorescence intensity as a function of the total ligand concentration was fitted to the experimental data points by means of non-linear, least-squares method, using Prism 3.02 (GraphPad Software, USA).

Thermofluor assays

Thermofluor assays were carried out using an RT–PCR instrument (Bio-Rad iCycler 5). The protein concentration used in this assay is 1 μM in the 20 mM HEPES buffer (pH 7.4) containing 100 mM KCl and 1 mM EDTA. The various caps were incubated with the protein for 10 min before the addition of SYPRO orange dye (1:1000 dilution) (Invitrogen). The fluorescence was measured with the increase of temperature at the rate of 1°C/min (excitation wavelength at 492 nm and emission wavelength at 610 nm). The data were analyzed using the Boltzmann equation in Prism 3.02 (GraphPad Software).

Accession numbers

Atomic coordinates and structure factors have been deposited in the Protein Data Bank for Ascaris eIF4E-3-m^7GTP-4E-BP complex (PDB code 3M93) and Ascaris eIF4E-3- $m^{2,2,7}$GTP-4E-BP complex (PDB code 3M94).

RESULTS

Structure of Ascaris eIF4E-3 in complex with m^7G-/$m^{2,2,7}$G-cap

Previous qualitative studies suggested that Ascaris eIF4E-3 recognizes both the m^7G and $m^{2,2,7}$G-cap (10), whereas studies on mammalian eIF4E proteins indicated they had very low affinity for $m^{2,2,7}$GTP (~100-fold less) compared with m^7GTP (16). We carried out quantitative fluorescent cap-binding studies with Ascaris eIF4E-3.

These studies suggested that Ascaris eIF4E-3 had equal affinity for m^7GpppG and $m^{2,2,7}$GpppG-cap (K_D = ~1 μM) (Table 1 and Supplementary Figure S1A). Sequence alignments comparing eIF4E proteins did not provide any obvious explanation for why the nematode proteins would have higher affinity for the $m^{2,2,7}$GpppG-cap compared with mammalian eIF4E (Supplementary Figure S1B).

In order to understand the binding mechanism of Ascaris eIF4E-3 with the $m^{2,2,7}$G-cap, we tried to determine the co-crystal structure of full-length Ascaris eIF4E-3 with the $m^{2,2,7}$G-cap. Full-length Ascaris eIF4E-3 with the $m^{2,2,7}$G-cap failed to produce diffraction quality crystals. Sequence alignment, trypsin digestion and isothermal titration calorimetry (ITC) cap-binding analyses indicated that N-terminal truncation of the protein (49–236) retained cap-binding ability (Table 2). Using this shorter construct in the presence of the human 4E-BP1 peptide, we obtained diffraction quality crystals and determined the co-crystal structures of Ascaris eIF4E-3 with $m^{2,2,7}$GTP and m^7GTP (Table 3). The overall structures of the Ascaris $m^{2,2,7}$GTP and m^7GTP complexes are very similar to each other (RMSD for Cα = 0.31 Å) and to the human eIF4E-m^7GTP complex structures (PDB: 2V8W, RMSD for Cα = 0.79 Å) (25) (Figure 1A–C and Supplementary Figure S1C). The human 4E-BP1 peptide binds to the opposite surface of the protein and forms interactions with Ascaris eIF4E-3 (Figure 1A and B) almost identical to those previously observed in the human eIF4E/4E-BP complex structure (43).

The electron density of both caps in the binding pocket is well defined except for the third phosphate (Figure 1D). Three main interactions occur between the $m^{2,2,7}$GTP-cap and the protein that include: (i) cation-π stacking between the guanine base and Trp69 and Trp115; (ii) electrostatic and hydrogen bonding interactions between Arg170 and Lys175 and the α and β phosphates of the $m^{2,2,7}$GTP-cap; and (iii) two H-bonds between the guanine N^1 and O^6 with the carboxyl group of Glu116 and the backbone amide of Trp115, respectively. Comparison of the Ascaris eIF4E-3 $m^{2,2,7}$GTP and m^7GTP complexes and other eukaryotic eIF4E complex structures (22,30) demonstrates that the only major difference on binding $m^{2,2,7}$G-cap is the loss of a single H-bond between the N^2 of the guanine base and the carboxyl group of Glu116 (Figure 1D).

To further evaluate the role of Glu116 in $m^{2,2,7}$GTP-cap binding, two mutants were generated (E116A and E116D). We predicted that the substitution of Glu by Asp or Ala would disrupt one H-bond between Glu carboxyl group and guanine N^2 of the m^7G-cap. However, the loss of the H-bond would not affect binding to the $m^{2,2,7}$GTP-cap since this H-bond is already absent, as shown in Figure 1D. The E116A substitution resulted in an insoluble protein precluding its use in cap-binding analysis. In contrast, the E116D substituted protein was readily purified. Binding studies using ITC demonstrated that the E116D substitution led to a decreased binding affinity for the m^7GTP-cap (10-fold), with little effect on $m^{2,2,7}$GTP-cap binding (Table 2). To examine the role of these substitutions on

Table 1. Fluorescent titration analysis of Ascaris eIF4E-3 and human eIF4E cap-binding affinity

Cap analog	K_D (μM)		ΔG° (kcal/mol)	
	Ascaris eIF4E-3	Human eIF4E (28–217)	Ascaris eIF4E-3	Human eIF4E (28–217)
m^7GTP	0.161 ± 0.005	0.0274 ± 0.0002	−9.11 ± 0.02	−10.138 ± 0.003
m^7GpppG[a]	0.787 ± 0.025	0.335 ± 0.036	−8.19 ± 0.03	−8.69 ± 0.06
$m^{2,2,7}$GpppG[a]	0.662 ± 0.057	3.1 ± 1.1	−8.28 ± 0.05	−7.38 ± 0.20
GTP	83 ± 14	140 ± 6[b]	−5.47 ± 0.10	−5.17 ± 0.03[b]
GpppG	116 ± 8	250 ± 19[b]	−4.87 ± 0.09	−4.43 ± 0.06[b]
GpppG[c]	232 ± 36	500 ± 38[b]		

[a]Results similar to these were obtained for m^7GpppA and $m^{2,2,7}$GpppA.
[b]Calculated from the values at 100 mM KCl and the slope of ionic-strength dependence of the association constants for the triphosphate mono- and dinucleotide cap analogs (16).
[c]Microscopic association constant derived from the measured one by dividing by a factor of two due to entropic effects for the symmetric cap analog.

Table 2. Isothermal titration calorimetry analysis of Ascaris eIF4E-3 and human eIF4E cap-binding affinity

Protein	Ligand	K_D (μM)	ΔH (kcal/mol)	TΔS (kcal/mol)	ΔG (kcal/mol)
Ascaris eIF4E-3	m^7GTP	0.24 ± 0.04	−14.5 ± 1.7	5.5 ± 1.4	−9.0
Ascaris eIF4E-3	$m^{2,2,7}$GTP	8.4 ± 1.0	−10.4 ± 0.3	3.54 ± 0.42	−6.86
Ascaris eIF4E-3 (49–236)	m^7GTP	0.17 ± 0.05	−12.38 ± 0.02	3.3 ± 0.56	−9.08
Ascaris eIF4E-3 (49–236)	$m^{2,2,7}$GTP	12.2 ± 3.9	−11.58 ± 0.52	5.02 ± 0.72	−6.56
Ascaris eIF4E-3 (E116D)	m^7GTP	1.98 ± 0.2	−11.04 ± 0.84	3.38 ± 0.78	−7.66
Ascaris eIF4E-3 (E116D)	$m^{2,2,7}$GTP	7.0 ± 0.1	−10.65 ± 0.05	3.69 ± 0.1	−6.96
Ascaris eIF4E-3 (49–236)	m^7GpppG	0.75 ± 0.19	−11.5 ± 0.8	3.3 ± 0.7	−8.2
Ascaris eIF4E-3 (49–236)	$m^{2,2,7}$GpppG[a]	17.2 ± 2.9	−4.52 ± 0.38	1.3 ± 0.1	−3.22
Human eIF4E	m^7GTP	0.032 ± 0.008	−12.54 ± 0.45	2.5 ± 0.3	−10.4
Human eIF4E	$m^{2,2,7}$GTP	4.56 ± 2.1	−12.1 ± 0.36	4.76 ± 1.01	−7.34

[a]Data were analyzed using the fixed stoichiometry (N = 1) due to the weak binding affinity (Supplementary Figure S1A).

Table 3. Crystal data and refinement statistics for Ascaris eIF4E-3

Data collection	m^7GTP-cap	$m^{2,2,7}$GTP-cap
Space group	I4 (1)	I4 (1)
Cell dimensions		
a (Å)	104.62	104.98
b (Å)	104.62	104.98
c (Å)	47.22	46.91
α (°)	90	90
β (°)	90	90
γ (°)	90	90
Measured reflections	22 966	104 640
Resolution[a]	39.99–2.9 (3.0–2.9)	41.73–2.00 (2.07–2.00)
R_{sym} or R_{merge}	0.113 (0.299)	0.113 (0.275)
I/σ	6.7 (2.2)	6.6 (3.2)
Completeness (%)	98.5 (98.8)	98.3 (98.1)
Redundancy	3.4 (3.3)	3.68 (3.7)
Refinement		
Resolution (Å)	2.9	2.05
Number of reflections	5713	15 993
R_{work}/R_{free}	23.6/29.8	20.4/24.4
Number of atoms		
Protein	1429	1441
Peptide	113	117
Ligand	29	31
Water	2	22
B factors		
Protein	45.6	21.4
Peptide	46.2	91.3
Ligand	77.5	41.6
Water	17	19.9
Rms deviations		
Bond length (Å)	0.011	0.01
Bond angles (°)	1.35	1.27
Ramachandran plot		
Residues in most favorable regions (%)	95.7	98.9
Residues in disallowed regions (%)	0	0

[a]Values in parentheses are for the highest resolution shell.

translation, we were able to functionally co-express both E116A and E116D with full-length Ascaris eIF4G and use them in translation assays. The substitutions in E116A or E116D led to a loss in translation of m^7G-capped mRNAs compared with $m^{2,2,7}$G-capped mRNAs (Figure 2A and B). Overall, these data are consistent with our structural observations indicating the importance of the hydrogen bonds at the N^2 position for binding of the m^7G-cap (16,22).

Characterization of Ascaris eIF4E-3 binding to m^7G- and $m^{2,2,7}$G-caps

A comparison of the Ascaris eIF4E-$m^{2,2,7}$G and Ascaris eIF4E-m^7G complexes presented here with the human eIF4E-m^7G complexes did not show any other major differences in the cap-binding pocket or the protein's interactions with the ligands (Supplemental Figure S1C). The two methyl groups at the N^2 position of the $m^{2,2,7}$G-cap are solvent exposed and have no apparent direct interaction with the protein. These observations suggest that mammalian eIF4E might be able to bind $m^{2,2,7}$G-cap with a similar binding affinity as that observed for the Ascaris eIF4E-3. In support of this prediction, both human eIF4E and Ascaris eIF4E-3 were retained on $m^{2,2,7}$GTP-sepharose and could be eluted by the $m^{2,2,7}$GTP-cap analog (Supplementary Figure S2A and S2B). We next carried out ITC binding studies on Ascaris and human eIF4E. These analyses indicated that Ascaris eIF4E-3 has a lower binding affinity for either $m^{2,2,7}$GTP or the $m^{2,2,7}$GpppG-cap compared with m^7GTP- and m^7GpppG caps (Table 2 and Supplementary Figure S2C–F). NMR studies of Ascaris eIF4E-3 with dinucleotide caps ($m^{2,2,7}$GpppG and m^7GpppG) further support that the affinity of Ascaris eIF4E-3 for $m^{2,2,7}$GpppG is lower than for m^7GpppG (Supplementary Figure S2G) as do SPR studies (data not shown). We note that while similar Ascaris eIF4E-3 binding affinities for the two caps were observed using fluorescence titration methods described above (Table 1), overall our interpretation of the structural, NMR and translation data (see below) are most consistent with the view that the affinity of Ascaris eIF4E-3 for the $m^{2,2,7}$G-cap is lower than for the m^7G-cap (see Discussion in Supplementary Data). Furthermore, the ITC data indicate that Ascaris eIF4E-3 and human eIF4E have similar and lower binding affinities for the $m^{2,2,7}$G-cap. Similar observations were made for eIF4E protein from the parasitic flatworm *Schistosoma mansoni* that also has $m^{2,2,7}$G-capped mRNAs (30). Thus, the major difference between the human, nematode and flatworm eIF4E is that the human protein has a higher binding affinity (6–9 fold) for m^7G-cap (Table 2) (14,30,44).

The lower binding affinity of mammalian eIF4E for the $m^{2,2,7}$GTP-cap was previously proposed to be a result of both a narrower binding pocket and steric hindrance caused by the two additional methyl groups at N^2 (14,15,29). Our structures of the Ascaris eIF4E-$m^{2,2,7}$G and eIF4E-m^7G suggest there is no direct interaction between the protein and the two methyl groups at the N^2 position. Furthermore, we have shown here that human and Ascaris eIF4E-3 have a similar affinity for the $m^{2,2,7}$GTP (Table 2 and Supplementary Figure S2). To examine if steric hindrance is responsible for the reduced affinity for the $m^{2,2,7}$G-cap, we tested the binding of a cap analog, bn^2m^7GMP (Supplementary Figure S3A), which has a large benzyl substituent at N^2 and find that it binds to both human and Ascaris eIF4E-3 with a 10-fold higher affinity compared with m^7GMP (Supplementary Table S1). These data suggest that additional N^2 methyl groups are not likely to preclude $m^{2,2,7}$GTP from entering the cap-binding pocket and that the pocket may be able to adapt its conformation to accommodate different caps. This is consistent with recent data indicating that the eIF4E cap binding pocket is relatively flexible (25). Further, as mammalian eIF4E undergoes a major conformational change on binding the cap (24,29,45), it is apparent that the N^2 substituent does not impede any conformational change required to form the cap-binding pocket or access of the cap to the pocket. Consistent with the increased affinity of bn^2m^7GMP for Ascaris eIF4E-3, it is also a strong competitive inhibitor of either m^7G- or $m^{2,2,7}$G-capped mRNA translation *in vitro* (Supplementary Figure S3B and S3C) and is a stronger inhibitor than m^7GTP. Furthermore, in an optimized cap-dependent rabbit

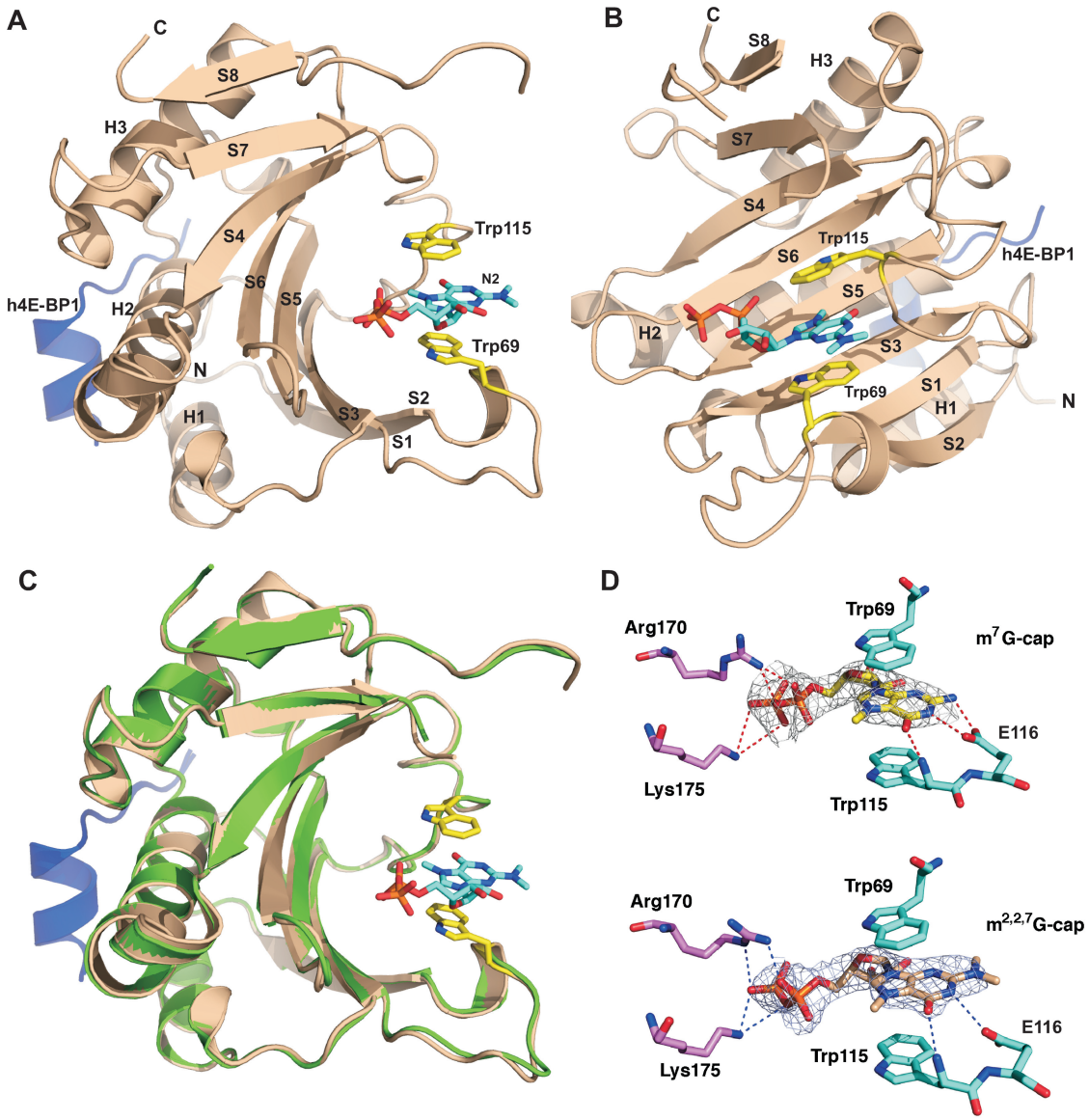

Figure 1. Structure comparison of Ascaris eIF4E-3 m^7GTP and $m^{2,2,7}$GTP complexes. (**A** and **B**) Ascaris eIF4E-3 structure in complex with $m^{2,2,7}$GTP and human 4E-BP1 peptide (blue) shown in two orientations. The three α helices and eight β strands in the structure are labeled. $m^{2,2,7}$GTP and the two stacking aromatic residues of eIF4E (Trp69 and Trp115—yellow) are shown as colored sticks. (**C**) Superimposition of Ascaris eIF4E-$m^{2,2,7}$GTP (Wheat) and m^7GTP-cap complexes (Green). The m^7GTP-cap is omitted from the figure. (**D**) m^7GTP and $m^{2,2,7}$GTP interactions in the Ascaris eIF4E-3 cap-binding pocket. The colored dashed lines illustrate hydrogen bonding. Note the additional hydrogen bond present with the m^7GTP-cap from E116. 2Fo-Fc Electron density map is contoured at a level of 1σ.

reticulocyte lysate translation system (Supplementary Figure S3D), addition of the benzyl group to m^7GMP significantly increases its efficacy as a translational inhibitor. Enhanced binding of eIF4E for bn^2m^7GMP may be due to a change in the methylated ring character (46) or an increased favorable entropy contribution from the N^2 benzyl group (47). The benzyl group of bn^2m^7GMP may form additional interactions with eIF4E to enhance cap binding.

eIF4E conformational differences on binding $m^{2,2,7}$G- versus m^7G-caps

To further explore the mechanistic basis for $m^{2,2,7}$G-cap binding, we used NMR chemical shift perturbation analyses to examine the changes that occur in Ascaris eIF4E-3 upon binding $m^{2,2,7}$G- and m^7G-caps (Supplementary Figure S4A). Approximately 25 residues from Ascaris eIF4E-3 exhibit significant chemical shift changes upon addition of m^7G- or $m^{2,2,7}$G-cap (Supplementary Figure S4B and S4D), indicating that these residues interact with the cap and/or undergo significant conformational rearrangements on binding the cap. These residues fall into three categories based on their location in the structure (Figure 3B): (i) residues involved in the formation of the cap-binding pocket or around the binding pocket; (ii) residues associated with the eIF4E/eIF4G interface (compare H1 and S2 in Figure 3B and D); and (iii) residues at a distance from these two

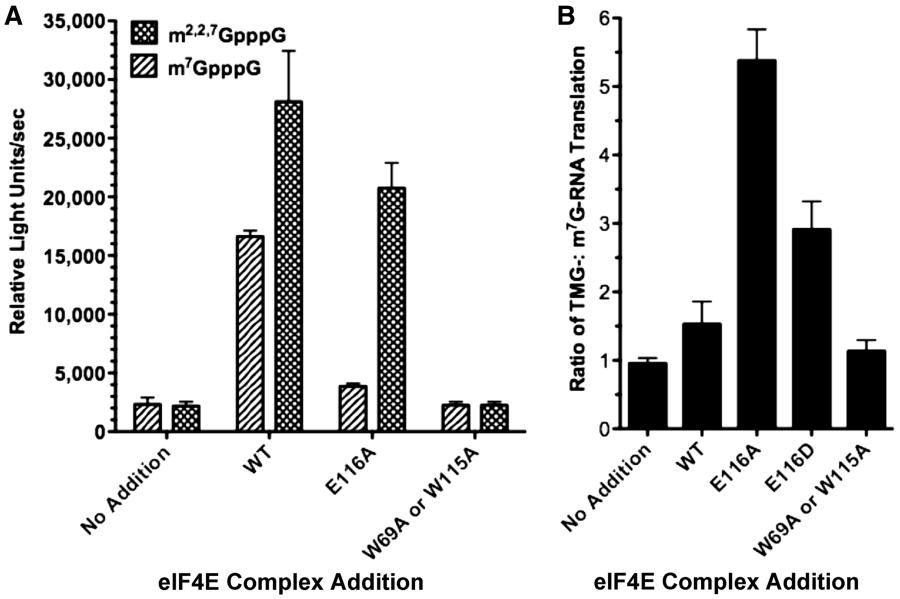

Figure 2. Mutations in Ascaris eIF4E-3 E116 have a greater affect on the translation of m^7G-capped compared with $m^{2,2,7}$-capped mRNAs. (**A**) Comparison of translation of m^7G- to $m^{2,2,7}G$-capped mRNAs by wild-type and mutant E116 eIF4E. W69A or W115A represent mutations in aromatic tryptophan residues required for cap binding and abolish translation. (**B**) Ratio of $m^{2,2,7}G$- to m^7G-capped mRNA translation as function of the wild-type and mutant E116 eIF4E. Ascaris embryo extracts were depleted of the eIF4F complex. eIF4F complex consisting of wild-type eIF4G and wild-type or mutant eIF4E complex were then added back to the extract to reconstitute translation as described (17).

regions. These data are consistent with chemical shift perturbations observed for the human eIF4E protein on binding m^7GTP-cap (24). The majority of residues with NMR chemical shift perturbations are similar on binding both the m^7G- and $m^{2,2,7}G$-cap (Supplementary Figure S4B–D), consistent with the minimal differences observed between the crystal structures of the eIF4E-$m^{2,2,7}G$ and eIF4E-m^7G complexes (Figure 1C).

However, there are clear differences in the magnitude of chemical shift changes on binding m^7G- versus $m^{2,2,7}G$-cap (Figure 3A–C). Most of the changes are significant reductions in the chemical shifts associated with residues located in and around the cap-binding pocket and near or at the eIF4E/eIF4G interface (see Figure 3D for cyan residues at the eIF4E/G interface). Reduced changes are observed in Lys112 and Asp117 (Figure 3A–B and Supplementary Figure S5) that may be a direct consequence of the loss of the H-bond between the N^2 of the base and carboxyl group of Glu116 on binding the $m^{2,2,7}G$-cap. Interactions with eIF4G may be affected by perturbations of residues Lys74, Gln75, Val76, Ala77 and Phe79 of S2 as well as Tyr104 (Figure 3B and C). These residues pack against alpha helix 1 and are connected to the key Trp69 that stacks with the methylated cap base (Figure 3C and D). Notably, both of these regions are part of the eIF4E interface with eIF4G. In addition, there are a number of changes at some distance from the binding pocket, including Asp157 that is also part of the eIF4E/G interface. Data examining mammalian eIF4E cap-binding (m^7GTP versus $m^{2,2,7}GTP$) conformation changes by increased susceptibility to pepsin cleavage showed conformational differences in regions of H1, H2 and S2 that support the changes we observe in the eIF4E/eIF4G interface on binding these two caps (29). While we envision potential networks of interactions that would lead to these changes emanating either from the alterations in Lys112 and Asp117 or residues adjacent to Trp69, peaks from a number of residues in the NMR spectra are missing or not assignable due to the effects of intermediate conformational exchange. Thus, the exact mechanism of how these perturbations are transmitted from the cap-binding pocket to these regions of Ascaris eIF4E-3 interface with eIF4G is unclear.

$m^{2,2,7}$GpppG-SL and eIF4E interaction reveals a possible explanation for the 'SL effect'

Nematode *trans*-splicing generates mRNAs with an $m^{2,2,7}$GpppG-cap followed by a conserved 22-nt RNA spliced leader. Translation of mRNA with only the $m^{2,2,7}$GpppG-cap is poor in nematodes (10,12). Efficient nematode translation of the $m^{2,2,7}$GpppG-capped mRNAs requires specific nucleotides and structural elements within the downstream spliced leader (SL) sequence including a stem loop that contains a 3-bp stem immediately following the cap (17). We have described this phenomenon as the 'SL effect'. The requirement for the SL in the translation of $m^{2,2,7}$GpppG-capped RNA appears consistent with the low affinity of Ascaris eIF4E-3 and the reduced conformational changes on binding this cap. We hypothesize that the SL is required to compensate for these deficiencies and facilitate translation. To examine where the SL might interact with Ascaris eIF4E-3, we used NMR spectroscopy to compare the binding of $m^{2,2,7}$GpppG-SL, $m^{2,2,7}$GpppG and $m^{2,2,7}GTP$-caps to Ascaris eIF4E-3. Comparison of the chemical shift perturbations in eIF4E on association with these three ligands (Figure 4A and B) demonstrated that the interaction with $m^{2,2,7}G$-SL leads to additional perturbation of residues around the cap-binding

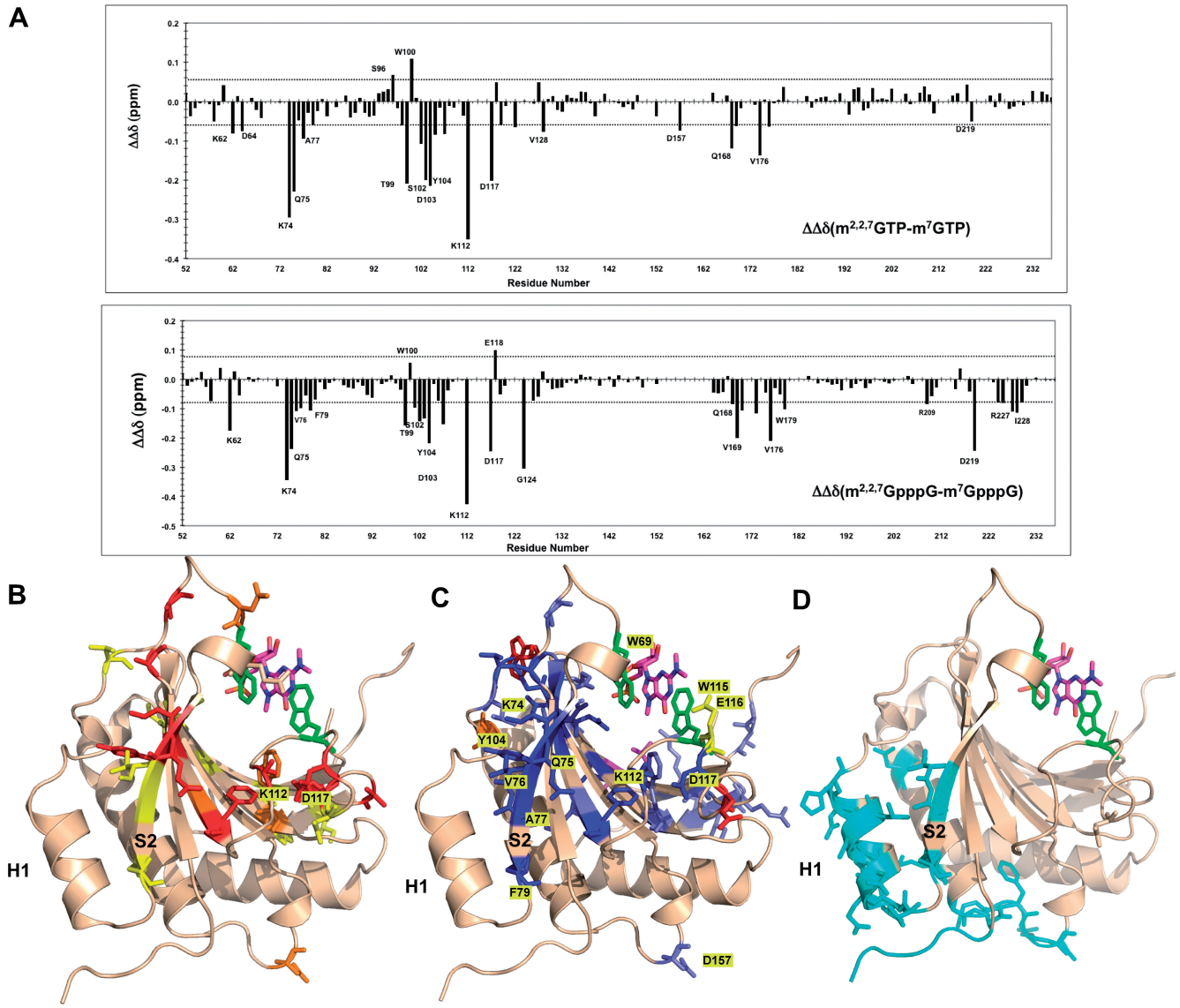

Figure 3. Ascaris eIF4E-3 chemical shift perturbations are less on binding the $m^{2,2,7}$G- compared to m^7G-cap. (**A**) Differences in eIF4E-3 chemical shift perturbation upon binding $m^{2,2,7}$G- compared to m^7G-cap. The reported difference in the chemical shift changes ($\Delta\Delta\delta$) is the difference in the weighted chemical shift changes, calculated as $\Delta\delta = \{\Delta\delta(^1H)^2 + 0.2 \times \Delta\delta(^{15}N)^2\}^{1/2}$, where $\Delta\delta(^1H)$ and $\Delta\delta(^{15}N)$ are the chemical-shift differences of the amide proton and nitrogen, relative to chemical shifts observed in the apo-protein, respectively (24,54). The dashed horizontal lines represent ±1 SD from the mean chemical shift difference. (**B**) Location of eIF4E-3 residues that show significant chemical shift perturbations on binding m^7GTP compared to the apo protein (Supplementary Figure S4A and S4B). Residues with major chemical shifts are colored as follows: red = >2.5 SD; orange = >2.0 SD; yellow = >1.5 SD above the mean. (**C**) Location of eIF4E-3 residues with significantly different chemical shift perturbations on binding $m^{2,2,7}$G- compared with the m^7G-cap. Data are derived from (A). Residues with major chemical shifts are colored as follows: red = chemical shifts >1 SD above the mean and blue = residues with chemical shift changes <1 SD below the mean. Orange (increase) and slate (decrease) residues are those that show less significant changes for one of the two comparisons ($m^{2,2,7}$GTP versus m^7GTP or $m^{2,2,7}$GpppG versus m^7GpppG).(**D**) Location of eIF4E-3 residues predicted to be involved in the interaction with eIF4G. eIF4E residues impacted by yeast eIF4G (393–490) (55) were mapped onto Ascaris eIF4E-3 and colored in cyan.

pocket (Gly101, Asp103, Val 128, Val 129, Val 167 and Asn168) and at the eIF4E/G interface including: (i) residues in the S2 strand (Lys75-Asp80) and (ii) residues in the H1 helix area (Glu83-Ala94). Unique chemical shift changes observed only in the presence of the SL occur in the region of Val128-Arg135 (Figure 4C). These perturbations may reflect the position of some portion of the SL RNA sequence on Ascaris eIF4E-3. Overall, these observations suggest that binding of $m^{2,2,7}$GpppG-SL may contribute to the structure or interactions within the cap-binding pocket and may influence Ascaris eIF4E-3 interactions with eIF4G and other translation factors through protein conformational changes (Figure 4B).

DISCUSSION

Spliced leader *trans*-splicing in metazoa generates mRNAs with an atypical mRNA-cap, $m^{2,2,7}$G-cap, followed by a

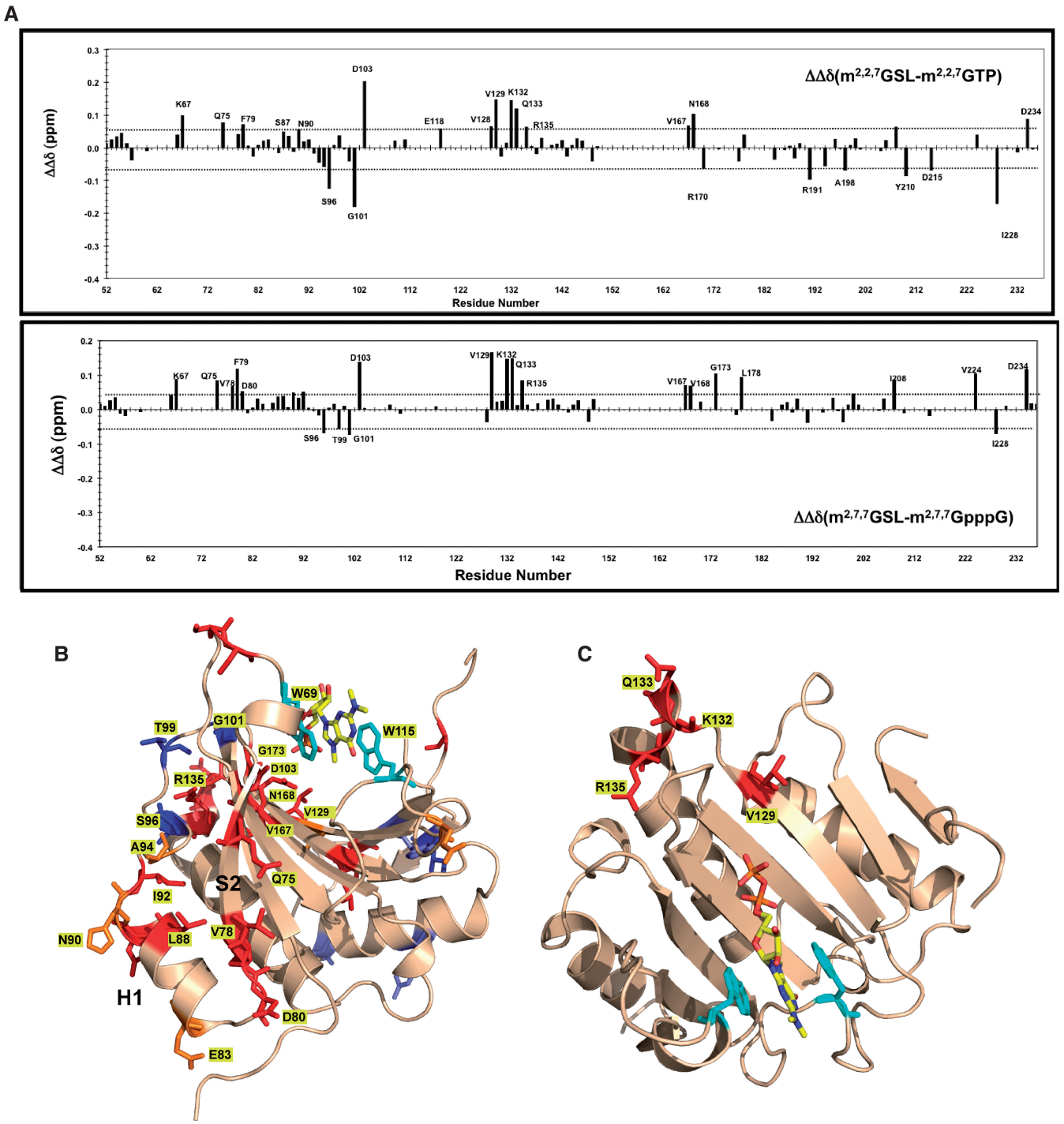

Figure 4. Chemical shift changes on Ascaris eIF4E-3 binding $m^{2,2,7}$G-spliced leader RNA increase changes at the eIF4E/G interface. (**A**) Chemical shift perturbations in eIF4E-3 on binding the $m^{2,2,7}$G-spliced leader RNA compared to either $m^{2,2,7}$GTP or $m^{2,2,7}$GpppG. Determined as described in Figure 3A. The dashed horizontal lines represent ±1 SD from the mean chemical shift difference. Residues with significant chemical shifts are colored as follows: red = chemical shifts >1 SD above the mean and blue = residues with chemical shift changes <1 SD below the mean. Orange residues represent residues that show smaller differences when comparing $m^{2,2,7}$GTP or $m^{2,2,7}$GpppG. (**B**) Location of eIF4E-3 residues with different significant chemical shift perturbations on binding $m^{2,2,7}$G-SL RNA compared to the $m^{2,2,7}$G-cap. Residues with major chemical shifts are colored as follows: red = chemical shifts >1 SD above the mean and blue = residues with chemical shift changes <1 SD below the mean. Orange residues represent residues that show less increased shifts or differences when comparing $m^{2,2,7}$GTP or $m^{2,2,7}$GpppG. (**C**) Location of residues that exhibit increased chemical shift perturbations only in the presence of the 22-nt SL-RNA. These regions do not show chemical shift changes in the presence of triphosphate or dinucleotide cap analogs and most likely represents a region that interacts with the SL-RNA.

spliced leader (9–12). In nematodes, two populations of mRNA are always present: (i) non-*trans*-spliced RNAs with a typical m^7GpppN-cap and variable 5′ sequence and (ii) *trans*-spliced RNAs with an $m^{2,2,7}$GpppG-cap and a common 22-nt 5′ spliced leader sequence. Ascaris eIF4E-3 can initiate the translation of both types of nematode mRNAs (17). Here, we describe the first structure of an eIF4E with an $m^{2,2,7}$G-cap and compare it to the cognate m^7G-eIF4E complex. These structures and NMR data indicate that the nematode *A. suum* eIF4E binds the two different caps in a similar manner except for the loss of a single hydrogen bond on binding the $m^{2,2,7}$G-cap. Consistent with the structures, both mammalian and nematode eIF4E have a similar low affinity for $m^{2,2,7}$G-cap compared with the m^7G-cap. The low affinity of eIF4E for the $m^{2,2,7}$G-cap is not a result of a narrower cap-binding pocket or steric hindrance as previously postulated. Nematode eIF4E binding to the m^7G-cap, $m^{2,2,7}$G-cap and $m^{2,2,7}$G-SL leads to distinct eIF4E conformational changes. Overall, these data lead us to propose a model for how the nematode spliced leader facilitates translation of $m^{2,2,7}$G-capped mRNAs.

Nematode eIF4E structure and conformation changes on cap binding

The overall structures of Ascaris eIF4E-3 bound to both caps are similar and resemble those determined for other eukaryotic eIF4E-cap complexes. (16,21–28). The major difference in Ascaris eIF4E-3 on binding $m^{2,2,7}$G-cap compared with the m^7G-cap is the loss of a single H-bond between the N^2 of the guanine base and the carboxyl group of Glu116 (Figure 1D), which leads to a significant drop in $m^{2,2,7}$G-cap binding affinity (Table 2). From ITC analysis, the reduced binding affinity for the $m^{2,2,7}$G-cap results from a reduced enthalpy (ΔH) presumably from the loss of the H-bond to Glu116, and also an increase in the unfavorable entropy. The crystal structures with the $m^{2,2,7}$G-cap and m^7G-cap reveal no significant differences in the crystallographic B-factors or atomic packing density in the vicinity of the ligand. However, formation of the H-bond between Glu116 and the N2 in the m^7G-cap would lead to release of water back into bulk solvent and would be entropically favorable. Therefore, the presence of the two methyl groups prevents this release, requires solvation of the exposed E116 side chain carboxyl, and additionally leads to increased solvent ordering around the two methyl groups leading to less favorable enthalpy.

Several lines of data suggest binding to the m^7G-cap compared with the $m^{2,2,7}$G-cap results in different protein conformations. First, although NMR spectroscopy reveals that most of the residues that change on binding each cap are the same, the magnitude of the chemical shift differences for a subset of these residues (20 of 25) is smaller on binding the $m^{2,2,7}$G-cap (Figure 3A and C). Second, the different entropy change on binding m^7GTP compared with $m^{2,2,7}$GTP (Table 2) further suggests that different protein conformational changes occur upon binding the different caps. Third, the thermafluor assays demonstrate that cap-binding stabilizes Ascaris eIF4E-3 against thermal denaturation and the stabilization is much greater with the m^7GTP compared with the $m^{2,2,7}$GTP-cap (Supplementary Figure S6). Overall, these data suggest that conformational changes are different on binding these two caps and these could have important ramifications in translation (see below).

Nematode eIF4E and the *trans*-spliced spliced leader

Efficient translation of $m^{2,2,7}$G-capped mRNAs in *Ascaris* requires specific sequence and structure within the downstream *trans*-spliced 22-nt SL sequence, the 'SL effect' (10,12,17). Notably, these SL elements do not facilitate translation of m^7G-capped RNAs in nematodes or $m^{2,2,7}$G-capped mRNAs in mammalian or plant translation systems (17). Furthermore, adaptations in the Ascaris eukaryotic translation initiation factor eIF4E/G complex enable efficient translation of the $m^{2,2,7}$G -SL RNAs in diverse *in vitro* translation systems (17).

One possible explanation for the requirement of the SL in the translation of $m^{2,2,7}$G-capped mRNAs is that the SL sequence facilitates or increases eIF4E-3 binding to the $m^{2,2,7}$G-cap. However, studies on Ascaris eIF4E-3 and eIF4E/G indicate that the SL sequence does not increase either Ascaris eIF4E-3 or eIF4E/G affinity for the $m^{2,2,7}$G-cap (17).

Our NMR data indicate that the SL leads to increased chemical shift changes in Ascaris eIF4E-3 S2 (Lys75-Asp80) and residues in the H1 helix region (Glu83-Ala94) (Figure 4A and B). Recent molecular dynamics data using *C. elegans* eIF4E isoforms also suggest that the flexible S1–S2 loop is affected by $m^{2,2,7}$G-cap binding (48). Residues located in S2 exhibit different chemical shifts upon interaction with the two caps. These chemical shifts are significantly less on binding the $m^{2,2,7}$G-cap (Figure 3A). We propose that binding of the m^7G-cap leads to perturbation of residues at the eIF4E/G interface (S2 and H1) (Figure 3B) and this is a result of a hydrogen bond interaction with Glu116, and possibly other changes. On binding the $m^{2,2,7}$G-cap, the loss of a hydrogen bond between the cap and Glu116 (and possibly other changes) leads to reduced changes in eIF4E at the interface of eIF4E with eIF4G. We propose that these interactions are required for recruitment of the 43S ribosome complex. When the $m^{2,2,7}$G-cap is bound, the loss of these interactions leads to reduced recruitment of the 43S ribosome complex. When the $m^{2,2,7}$G-cap is present with the SL, the SL leads to increased chemical shift changes including those in S2 (Lys75-Asp80) and residues in the H1 helix region (Glu83-Ala94) at the eIF4E/G interface. Therefore, we propose that the SL sequence in the $m^{2,2,7}$G-capped RNA is required to induce the requisite conformational changes necessary for interactions at the Ascaris eIF4E/eIF4G interface. The reduced binding affinity of nematode eIF4E for m^7G-cap compared with human eIF4E may allow additional degrees of conformational flexibility in Ascaris eIF4E-3 that enable alternate conformations of the eIF4E/G/cap ternary complex necessary for translation of the two populations of mRNAs (m^7G- and

$m^{2,2,7}$G-capped) in nematodes. Additional adaptations in the Ascaris eIF4E/G are also required (17).

Nematode eIF4E cap binding specificity

Our initial interest in determining the structure of Ascaris eIF4E-3 was based on the premise that Ascaris eIF4E-3 and eIF4E from other metazoa with *trans*-splicing had adaptations in their eIF4Es to specifically recognize the $m^{2,2,7}$G-cap (10,13–16,30,44). However, our new data demonstrate that both human and Ascaris eIF4E-3 recognize the $m^{2,2,7}$G-cap with broadly similar, but low affinity, and that the major difference in cap-binding between the Ascaris and human proteins is the higher affinity of the human protein for the m^7G-cap (Table 2 and Discussion in Supplementary Data).

The lower binding affinity of mammalian eIF4E for the $m^{2,2,7}$GTP-cap was previously proposed to be a result of both a narrower binding pocket and steric hindrance due to the introduction of two additional methyl groups at N^2, thus preventing this cap from entering the cap binding pocket (14,15,29). However, our structures of the Ascaris eIF4E-$m^{2,2,7}$G and eIF4E-m^7G complexes rule this out as there is no direct interaction between the protein and the two methyl groups at N^2 in the base (Figure 1). We show that both human and Ascaris eIF4E-3 have a similar affinity for the $m^{2,2,7}$GTP (Table 2 and Supplementary Figure S2). In addition, the cap analog, bn^2m^7GMP, with a large benzyl substituent at N^2 position, has increased binding affinity to both Ascaris and human eIF4E further suggesting that the N^2 substituent does not impede the known eIF4E conformational change required to form the cap binding pocket or prevent access of the cap to the pocket. Our observation that addition of an N^2 benzyl group substituent on a monophosphate (this bn^2m^7GMP) is a better ligand for mammalian eIF4E and leads to significant translation inhibition may provide a novel avenue for cap analog inhibitor development (Supplementary Figure S3D).

Five isoforms of eIF4E have been described in *C. elegans* (13,15,49) with two isoforms, described as primarily specific for the m^7G-cap, whereas the remaining three interact with both the m^7G- and $m^{2,2,7}$G-caps. Mutagenesis studies on the *C. elegans* dual cap-binding protein eIF4E-5 suggested that alteration of two specific residues (N64Y/V65L) led to a 2-fold decrease in binding specificity for $m^{2,2,7}$GTP-cap (14). These substitutions were suggested to influence both the width and depth of the cap-binding pocket. However, native Ascaris eIF4E-3 has both of these substitutions (Tyr105 and Leu106) (10). The position of these two residues in the Ascaris eIF4E-3 complex structures (m^7GTP or $m^{2,2,7}$GTP-cap) and their lack of change on binding the two caps (Supplementary Figure S7) suggests they are not likely the key determinants of cap binding specificity.

The only other trimethylguanosine cap-binding protein whose structure is known is snurportin1 (PDB: 1XK5) (46). Snurportin specifically binds the trimethylguanosine cap of snRNAs. The $m^{2,2,7}$GpppG-cap-binding mechanism for snurportin1 (PDB:1XK5) is different from that observed in Ascaris eIF4E-3 (Supplementary Figure S8). The hypermethylated base of the cap is stacked with an aromatic group (Trp107) of snurportin and the second base forms the third residue in a stacked sandwich. Consistent with this structure, snurportin binds a dinucleotide cap ($m^{2,2,7}$GpppG) with a 10-fold higher affinity than a mononucleotide cap (46). While the methyl group at N^7 introduces a net positive charge into the guanine ring and thus enhances the stacking energy between the base and eIF4E Trp (16), the two additional methyl groups at the exocyclic N^2 have been proposed to have no effect on the stacking interaction (50). Thus, the two additional methyl groups at N^2 of the cap appear to play very different roles in their interaction with eIF4E compared with snuportin1 where they form a hydrophobic interaction with Trp107 (Supplementary Figure S8).

CONCLUSIONS

Our data provide new insight into the mechanism of eIF4E binding to the atypical $m^{2,2,7}$G mRNA cap, identify eIF4E conformational changes on binding m^7G and $m^{2,2,7}$G mRNA caps, and suggest a key interaction between the *trans*-spliced nematode 5′-UTR and eIF4E necessary for efficient translation of *trans*-spliced mRNAs in nematodes. Some mammalian mRNAs are more dependent on eIF4E levels or eIF4E cap affinity for efficient translation (51–53). Given our data, we suggest that eIF4E binding to the cap may be dependent on or influenced by the RNA 5′-UTR sequence and structure and that this may influence translation efficiency of some eukaryotic mRNAs.

Most eukaryotes have several isoforms of eIF4E (6,28). Alignment of eIF4E isoform sequences and residues associated with their cap-binding pockets indicates that most are very similar. However, based on our findings, inherent differences in eIF4E isoform protein flexibility, ternary complex formation and interaction with the mRNA 5′-UTR may have important consequences in translation initiation resulting in distinct physiological roles for eIF4E isoforms in translation of different mRNAs.

ACCESSION NUMBERS

3M93, 3M94.

SUPPLEMENTARY DATA

Supplementary Data are available at NAR Online.

ACKNOWLEDGEMENTS

We thank Katherine Borden for providing human eIF4E and NMR data, Shaun Bevers at the University of Colorado Denver biophysical core for help with ITC, and members of the structural biology community at the University of Colorado Denver School of Medicine, University of Colorado Denver X-ray and NMR facility (supported in part by the University of Colorado Cancer Center). We thank Katherine Borden, Laurent Volpon,

and members of the Davis lab for their comments on the article.

FUNDING

National Institutes of Health grants (AI049558 and AI080805 to R.E.D); Howard Hughes Medical Institute Grant (55005604 to E.D.); Polish Ministry of Science and Higher Education grant (N N301 267 137 to A.N.), (N N301 035 936 to R.S.), (N N301 096339 to E.D.). Funding for open access charge: National Institutes of Health.

Conflict of interest statement. None declared.

REFERENCES

1. Mathews,M.B., Sonenberg,N. and Hershey,J. (2007) Origins and principles of translational control. In Mathews,M.B., Sonenberg,N. and Hershey,J. (eds), *Translational Control in Biology and Medicine*. Cold Spring Harbor Press, Cold Spring Harbor, pp. 1–40.
2. Sonenberg,N. and Hinnebusch,A.G. (2009) Regulation of translation initiation in eukaryotes: mechanisms and biological targets. *Cell*, **136**, 731–745.
3. Jackson,R.J., Hellen,C.U. and Pestova,T.V. (2010) The mechanism of eukaryotic translation initiation and principles of its regulation. *Nat. Rev. Mol. Cell. Biol.*, **11**, 113–127.
4. Gingras,A.-C., Raught,B. and Sonenberg,N. (1999) eIF4 initiation factors: effectors of mrna recruitment to ribosomes and regulators of translation. *Ann. Rev. Biochem.*, **68**, 913–963.
5. Von Der Haar,T., Gross,J.D., Wagner,G. and McCarthy,J.E. (2004) The mRNA cap-binding protein eIF4E in post-transcriptional gene expression. *Nat. Struct. Mol. Biol.*, **11**, 503–511.
6. Rhoads,R.E. (2009) eIF4E - new family members, new binding partners, new roles. *J. Biol. Chem.*, **284**, 16711–16715.
7. Darzynkiewicz,E., Stepinski,J., Ekiel,I., Goyer,C., Sonenberg,N., Temeriusz,A., Jin,Y., Sijuwade,T., Haber,D. and Tahara,S.M. (1989) Inhibition of eukaryotic translation by nucleoside 5′-monophosphate analogues of mRNA 5′-cap: changes in N7 substituent affect analogue activity. *Biochemistry*, **28**, 4771–4778.
8. Cai,A., Jankowska-Anyszka,M., Centers,A., Chlebicka,L., Stepinski,J., Stolarski,R., Darzynkiewicz,E. and Rhoads,R.E. (1999) Quantitative assessment of mRNA cap analogues as inhibitors of in vitro translation. *Biochemistry*, **38**, 8538–8547.
9. Allen,M.A., Hillier,L.W., Waterston,R.H. and Blumenthal,T. (2011) A global analysis of C. elegans trans-splicing. *Genome Res.*, **21**, 255–264.
10. Lall,S., Friedman,C.C., Jankowska-Anyszka,M., Stepinski,J., Darzynkiewicz,E. and Davis,R.E. (2004) Contribution of trans-splicing, 5′ -leader length, cap-poly(A) synergism, and initiation factors to nematode translation in an Ascaris suum embryo cell-free system. *J. Biol. Chem.*, **279**, 45573–45585.
11. Liou,R.F. and Blumenthal,T. (1990) Trans-spliced Caenorhabditis elegans mRNAs retain trimethylguanosine caps. *Mol. Cell. Biol.*, **10**, 1764–1768.
12. Maroney,P.A., Denker,J.A., Darzynkiewicz,E., Laneve,R. and Nilsen,T.W. (1995) Most mRNAs in the nematode Ascaris lumbricoides are trans-spliced: a role for spliced leader addition in translational efficiency. *RNA*, **1**, 714–723.
13. Jankowska-Anyszka,M., Lamphear,B.J., Aamodt,E.J., Harrington,T., Darzynkiewicz,E., Stolarski,R. and Rhoads,R.E. (1998) Multiple isoforms of eukaryotic protein synthesis initiation factor 4E in C.elegans can distinguish between mono- and trimethylated mRNA cap structures. *J. Biol. Chem.*, **273**, 10538–10542.
14. Miyoshi,H., Dwyer,D.S., Keiper,B.D., Jankowska-Anyszka,M., Darzynkiewicz,E. and Rhoads,R.E. (2002) Discrimination between mono- and trimethylated cap structures by two isoforms of Caenorhabditis elegans eIF4E. *EMBO J.*, **21**, 4680–4690.
15. Keiper,B.D., Lamphear,B.J., Deshpande,A.M., Jankowska-Anyszka,M., Aamodt,E.J., Blumenthal,T. and Rhoads,R.E. (2000) Functional characterization of five eIF4E isoforms in Caenorhabditis elegans. *J. Biol. Chem.*, **275**, 10590–10596.
16. Niedzwiecka,A., Marcotrigiano,J., Stepinski,J., Jankowska-Anyszka,M., Wyslouch-Cieszynska,A., Dadlez,M., Gingras,A.C., Mak,P., Darzynkiewicz,E., Sonenberg,N. *et al.* (2002) Biophysical studies of eIF4E cap-binding protein: recognition of mRNA 5′ cap structure and synthetic fragments of eIF4G and 4E-BP1 proteins. *J. Mol. Biol.*, **319**, 615–635.
17. Wallace,A., Filbin,M.E., Veo,B., McFarland,C., Stepinski,J., Jankowska-Anyszka,M., Darzynkiewicz,E. and Davis,R.E. (2010) The nematode eukaryotic translation initiation factor 4E/G complex works with a trans-spliced leader stem-loop to enable efficient translation of trimethylguanosine-capped RNAs. *Mol. Cell Biol.*, **30**, 1958–1970.
18. Darzynkiewicz,E., Stepinski,J., Ekiel,I., Jin,Y., Haber,D., Sijuwade,T. and Tahara,S.M. (1988) Beta-globin mRNAs capped with m7G, m2.7(2)G or m2.2.7(3)G differ in intrinsic translation efficiency. *Nucleic Acids Res.*, **16**, 8953–8962.
19. Ferguson,K.C., Heid,P.J. and Rothman,J.H. (1996) The SL1 trans-spliced leader RNA performs an essential embryonic function in Caenorhabditis elegans that can also be supplied by SL2 RNA. *Genes Dev.*, **10**, 1543–1556.
20. Hotez,P.J. (2008) Neglected infections of poverty in the United States of america. *PLoS Negl. Trop. Dis.*, **2**, e256.
21. Matsuo,H., Li,H., McGuire,A.M., Fletcher,C.M., Gingras,A.C., Sonenberg,N. and Wagner,G. (1997) Structure of translation factor eIF4E bound to m7GDP and interaction with 4E-binding protein. *Nat. Struct. Biol.*, **4**, 717–724.
22. Marcotrigiano,J., Gingras,A.C., Sonenberg,N. and Burley,S.K. (1997) Cocrystal structure of the messenger RNA 5′ cap-binding protein (eIF4E) bound to 7-methyl-GDP. *Cell*, **89**, 951–961.
23. Monzingo,A.F., Dhaliwal,S., Dutt-Chaudhuri,A., Lyon,A., Sadow,J.H., Hoffman,D.W., Robertus,J.D. and Browning,K.S. (2007) The structure of eukaryotic translation initiation factor-4E from wheat reveals a novel disulfide bond. *Plant Physiol.*, **143**, 1504–1518.
24. Volpon,L., Osborne,M.J. and Borden,K.L. (2006) NMR assignment of human eukaryotic translation initiation factor 4E (eIF4E) in its cap-free form. *J. Biomol. NMR*, **36(Suppl. 1)**, 65.
25. Brown,C.J., McNae,I., Fischer,P.M. and Walkinshaw,M.D. (2007) Crystallographic and mass spectrometric characterisation of eIF4E with N7-alkylated cap derivatives. *J. Mol. Biol.*, **372**, 7–15.
26. Tomoo,K., Shen,X., Okabe,K., Nozoe,Y., Fukuhara,S., Morino,S., Ishida,T., Taniguchi,T., Hasegawa,H., Terashima,A. *et al.* (2002) Crystal structures of 7-methylguanosine (m7GTP)- and P1-7-methylguanosine-P3-adenosine-5′, 5′-triphosphate (m7GpppA)-bound human full-length eukaryotic initiation factor 4E: biological importance of the C-terminal flexible region. *Biochem. J.*, **362**, 539–544.
27. Tomoo,K., Shen,X., Okabe,K., Nozoe,Y., Fukuhara,S., Morino,S., Sasaki,M., Taniguchi,T., Miyagawa,H., Kitamura,K. *et al.* (2003) Structural features of human initiation factor 4E, studied by X-ray crystal analyses and molecular dynamics simulations. *J. Mol. Biol.*, **328**, 365–383.
28. Rosettani,P., Knapp,S., Vismara,M.G., Rusconi,L. and Cameron,A.D. (2007) Structures of the human eIF4E homologous protein, h4EHP, in its m7GTP-bound and unliganded forms. *J. Mol. Biol.*, **368**, 691–705.
29. Rutkowska-Wlodarczyk,I., Stepinski,J., Dadlez,M., Darzynkiewicz,E., Stolarski,R. and Niedzwiecka,A. (2008) Structural changes of eIF4E upon binding to the mRNA 5′ monomethylguanosine and trimethylguanosine cap. *Biochemistry*, **47**, 2710–2720.
30. Liu,W., Zhao,R., McFarland,C., Kieft,J., Niedzwiecka,A., Jankowska-Anyszka,M., Stepinski,J., Darzynkiewicz,E., Jones,D.N. and Davis,R.E. (2009) Structural insights into parasite eIF4E binding specificity for m7G and m2,2,7G mRNA caps. *J. Biol. Chem.*, **284**, 31336–31349.
31. Darzynkiewicz,E., Ekiel,I., Tahara,S.M., Seliger,L.R. and Shatkin,A.J. (1985) Chemical synthesis and characterization of 7-methylguanosine cap analogs. *Biochemistry*, **24**, 1701–1707.

32. Jankowska,M., Temeriusz,A., Stolarski,R. and Darzynkiewicz,E. (1993) Synthesis of m2,7GTP- and m2,2,7GTP-sepharose 4B: new affinity resins for isolation of cap binding proteins. *Collect. Czech. Chem. Commun.*, **58**, 132–137.
33. Stepinski,J., Bretner,M., Jankowska,M., Felczak,K., Stolarski,R., Wieczorek,Z., Cai,A.-L., Rhoads,R.E., Temeriusz,A., Haber,D. *et al.* (1995) Synthesis and properties of P1,P2-, P1,P3- and P1,P4-dinucleoside di-, tri- and tetraphosphate mRNA 5′-cap analogues. *Nucleosides Nucleotides*, **14**, 717–721.
34. Avino,A.M., Espuny,R., Bach,M. and Eritja,R. (1995) A convenient method for the preparation of N2,N2-dimethylguanosine. *Nucleosides Nucleotides*, **7**, 1613–1617.
35. Yoshikawa,M., Kato,T. and Takenishi,T. (1967) A novel method for phosphorylation of nucleosides to 5′-nucleotides. *Tetrahedron Lett.*, **8**, 5065–5068.
36. CCP4. (1994) The CCP4 suite: programs for protein crystallography. *Acta Crystallogr. D Biol. Crystallogr.*, **50**, 760–763.
37. Emsley,P. and Cowtan,K. (2004) Coot: model-building tools for molecular graphics. *Acta Crystallogr. D Biol. Crystallogr.*, **60(Pt 12 Pt 1)**, 2126–2132.
38. Delano,W.L. (2002) *The Pymol Molecular Graphics System*. Delano Scientific, San Carlos, CA.
39. Painter,J. and Merritt,E.A. (2006) Optimal description of a protein structure in terms of multiple groups undergoing TLS motion. *Acta Crystallogr. D Biol. Crystallogr.*, **62(Pt 4)**, 439–450.
40. Delaglio,F., Grzesiek,S., Vuister,G.W., Zhu,G., Pfeifer,J. and Bax,A. (1995) NMRPipe: a multidimensional spectral processing system based on UNIX pipes. *J. Biomol. NMR*, **6**, 277–293.
41. Vranken,W.F., Boucher,W., Stevens,T.J., Fogh,R.H., Pajon,A., Llinas,M., Ulrich,E.L., Markley,J.L., Ionides,J. and Laue,E.D. (2005) The CCPN data model for NMR spectroscopy: development of a software pipeline. *Proteins*, **59**, 687–696.
42. Kowalska,J., Lukaszewicz,M., Zuberek,J., Ziemniak,M., Darzynkiewicz,E. and Jemielity,J. (2009) Phosphorothioate analogs of m7GTP are enzymatically stable inhibitors of cap-dependent translation. *Bioorg. Med. Chem. Lett.*, **19**, 1921–1925.
43. Marcotrigiano,J., Gingras,A.C., Sonenberg,N. and Burley,S.K. (1999) Cap-dependent translation initiation in eukaryotes is regulated by a molecular mimic of eIF4G. *Mol. Cell*, **3**, 707–716.
44. Stachelska,A., Wieczorek,Z., Ruszczynska,K., Stolarski,R., Pietrzak,M., Lamphear,B.J., Rhoads,R.E., Darzynkiewicz,E. and Jankowska-Anyszka,M. (2002) Interaction of three Caenorhabditis elegans isoforms of translation initiation factor eIF4E with mono- and trimethylated mRNA 5′ cap analogues. *Acta Biochim. Pol.*, **49**, 671–682.
45. Niedzwiecka,A., Darzynkiewicz,E. and Stolarski,R. (2004) Thermodynamics of mRNA 5′ cap binding by eukaryotic translation initiation factor eIF4E. *Biochemistry*, **43**, 13305–13317.
46. Strasser,A., Dickmanns,A., Luhrmann,R. and Ficner,R. (2005) Structural basis for m3G-cap-mediated nuclear import of spliceosomal UsnRNPs by snurportin1. *EMBO J.*, **24**, 2235–2243.
47. Zidek,L., Novotny,M.V. and Stone,M.J. (1999) Increased protein backbone conformational entropy upon hydrophobic ligand binding. *Nat. Struct. Biol.*, **6**, 1118–1121.
48. Ruszczynska-Bartnik,K., Maciejczyk,M. and Stolarski,R. (2011) Dynamical insight into Caenorhabditis elegans eIF4E recognition specificity for mono-and trimethylated structures of mRNA 5′ cap. *J. Mol. Mod.*, **17**, 727–737.
49. Amiri,A., Keiper,B.D., Kawasaki,I., Fan,Y., Kohara,Y., Rhoads,R.E. and Strome,S. (2001) An isoform of eIF4E is a component of germ granules and is required for spermatogenesis in C. elegans. *Development*, **128**, 3899–3912.
50. Ruszczynska,K., Kamienska-Trela,K., Wojcik,J., Stepinski,J., Darzynkiewicz,E. and Stolarski,R. (2003) Charge distribution in 7-methylguanine regarding cation-pi interaction with protein factor eIF4E. *Biophys. J.*, **85**, 1450–1456.
51. De Benedetti,A. and Graff,J.R. (2004) eIF-4E expression and its role in malignancies and metastases. *Oncogene*, **23**, 3189–3199.
52. Koromilas,A.E., Lazaris-Karatzas,A. and Sonenberg,N. (1992) mRNAs containing extensive secondary structure in their 5′ non-coding region translate efficiently in cells overexpressing initiation factor eIF-4E. *EMBO J.*, **11**, 4153–4158.
53. Mamane,Y., Petroulakis,E., Martineau,Y., Sato,T.A., Larsson,O., Rajasekhar,V.K. and Sonenberg,N. (2007) Epigenetic activation of a subset of mRNAs by eIF4E explains its effects on cell proliferation. *PLoS ONE*, **2**, e242.
54. Grzesiek,S., Stahl,S.J., Wingfield,P.T. and Bax,A. (1996) The CD4 determinant for downregulation by HIV-1 Nef directly binds to Nef. Mapping of the Nef binding surface by NMR. *Biochemistry*, **35**, 10256–10261.
55. Gross,J.D., von Moerke,N.J., der Haar,T., Lugovsky,A.A., Sachs,A.B., McCarthy,J.E.G. and Wagner,G. (2003) Ribosome Loading onto the mRNA cap is driven by conformational coupling between eIF4G and eIF4E. *Cell*, **115**, 739–750.